ELSEVIER

International Journal of Mass Spectrometry 192 (1999) 259–266

International Journal of Mass Spectrometry

Multifragmentation after multi-ionization of hydrogen clusters in high energy cluster–atom and cluster–cluster collisions

B. Farizon, M. Farizon*, M.J. Gaillard

Institut de Physique Nucléaire de Lyon, IN2P3-CNRS et Université Claude Bernard, 43, boulevard du 11 Novembre 1918, F-69622 Villeurbanne Cedex, France

Received 8 January 1999; accepted 19 March 1999

Abstract

We report on a cluster fragmentation study involving collisions of high-energy hydrogen cluster ions with atomic helium or fullerenes. The experimental characterization of the cluster fragmentation, not only by the average fragment size distribution but also by a statistical analysis of the fragmentation events, has become possible because of a recently developed multicoincidence technique in which all the fragments of all the collisions occurring in the experiment are mass analyzed on an event by event basis. From the breakup in two fragments to the complete disintegration of the cluster, the fragmentation phenomenon exhibits a transition with an increase of the fluctuations. The fragmentation events with more than one H_3^+ fragment evidence the cluster multifragmentation process. An important aspect of these results is that high-energy cluster collision can induce a reaction in the cluster. (Int J Mass Spectrom 192 (1999) 259–266) © 1999 Elsevier Science B.V.

Keywords: High-energy collisions; Hydrogen cluster ions; Cluster multifragmentation; Cluster multi-ionization; Phase transition; Critical behaviour; Cluster–cluster collisions

1. Introduction

Fragmentation [1] covers a wide range of phenomena in science and technology, i.e. polymer, colloids, droplets, rocks, etc., and studies are developing rapidly in quite different areas such as subatomic particles, soft matter, and materials. In addition, fragmentation of atomic nuclei will likely become an effective way of handling nuclear waste.

Despite intensive research in various fields of science and technology, complete analysis and understanding of fragmentation has not yet been achieved. Nevertheless, there is the recognition that general features of this phenomenon are rather independent of the actual system and its underlying interaction forces. Thus it is highly desirable to be able to study a model system in as much detail as possible in order to arrive at sound conclusions that may be applied (and compared) to a larger range of objects. Clusters that are aggregates of atoms or molecules in the form of microscopic and submicroscopic particles have revealed themselves to be an appropriate system. The hydrogen cluster ions are the simplest ionized molecular complexes that have attracted experimental efforts to clarify their structure and properties for decades [2]. A number of experiments suggest that their structure consists of a tightly bound H_3^+ core ion

* Corresponding author. E-mail: bfarizon@ipnl.in2p3.fr

PII S1387-3806(99)00091-3

solvated by more weakly bound H_2 molecules that are symmetrically arranged in solvation shells around the core in striking difference to the structure of the neutral clusters. Recent quantum Monte Carlo simulation [3] and quantum chemical calculations [4] have investigated the effect of protonation of pure hydrogen clusters $(H_2)_n$ at low temperatures. It was shown that the added proton gets trapped as a very localized and strongly bound H_3^+ impurity in the cluster core surrounded by stable shells of more spatially delocalized solvating H_2 molecules.

For fragmentation phenomena a natural classification should involve the fragmentation size distribution. These fragment size distributions often show a structure that may depend on external control parameters like the available energy, the density of the system, etc. Thus, researchers in many fields are confronted with the need to characterize the data in a meaningful way and to determine the dynamical processes that cause fragmentation. High energy cluster–atom or cluster–cluster collision experiments in which all fragments issued from a particular collision are detected in the coincidence mode can provide valuable information to test the predictions of general models describing fragmentation phenomena.

Here, we report on a cluster fragmentation study involving collisions of high energy hydrogen cluster ions with atomic helium or fullerenes in which all the fragments of all the collisions occurring in the experiment are mass analysed on an event by event basis using a novel multicoincidence technique.

2. Experimental setup

Mass selected hydrogen cluster ions of 60 keV/u are delivered by the cluster facility of the IPN Lyon consisting of a cryogenic cluster jet expansion source combined with a high-performance electron ionizer and a two-step ion accelerator (for details see [5,6]. After momentum analysis by a magnetic field, the mass selected and pulsed high-energy projectile beam (pulse length of 100 ms, repetition frequency of 1 Hz) is collimated by two apertures ensuring an angular dispersion of about ± 0.8 mrad. This cluster ion projectile beam is crossed perpendicularly by a helium gas jet [7] or by a C_{60} effusive beam produced by evaporation of pure C_{60} powder in a single-chamber molybdenum oven (at about 675 °C). Fig. 1 shows a schematic view of the experimental setup for the C_{60} target case.

One meter behind the interaction region the fast hydrogen products (neutral and ions) pass a magnetic sector field analyzer. The charged and neutral fragments are then detected with a multidetector device consisting of several surface barrier detectors located at different angular positions at the exit of the analyzer. The peak amplitude of the signals given by the detectors is coded with an AD413A module (EG&G ORTEC, Oak Ridge, TN) used in the coincidence mode. A master gate signal derived from the signal given by the detectors causes several analog inputs to be grouped as a set of coincident events. Each set of coincident events is saved as a fragmentation event and can be sorted using various conditions. The width of the master gate pulse is 2.5 ms and the intensity of the cluster beam is lowered to 1000 clusters per second to avoid fragmentation of two incident clusters during this time window.

This allows one to simultaneously record neutral and charged fragments detected in coincidence for each single event irrespective of the nature of the collisional interaction, i.e. small or large impact parameters leading to rather “gentle” or “violent” collisions. Moreover, in this experimental situation, during the collisional interaction the energy is deposited in a short time compared to the typical time of the internal motion of the cluster components. Therefore, in each case the excitation can be thought of as being due to perturbation followed by the cluster fragmentation governed by the energy deposited.

3. Size distributions of the charged fragments

Fig. 2(a) shows the fragment ion yield Y_p (i.e. number of each fragment ion H_p^+ divided by the total number of fragment ions per reactive collision) versus the fragment size p ($p = 3$–23, odd) resulting from the fragmentation of H_{25}^+ colliding with helium or C_{60}.

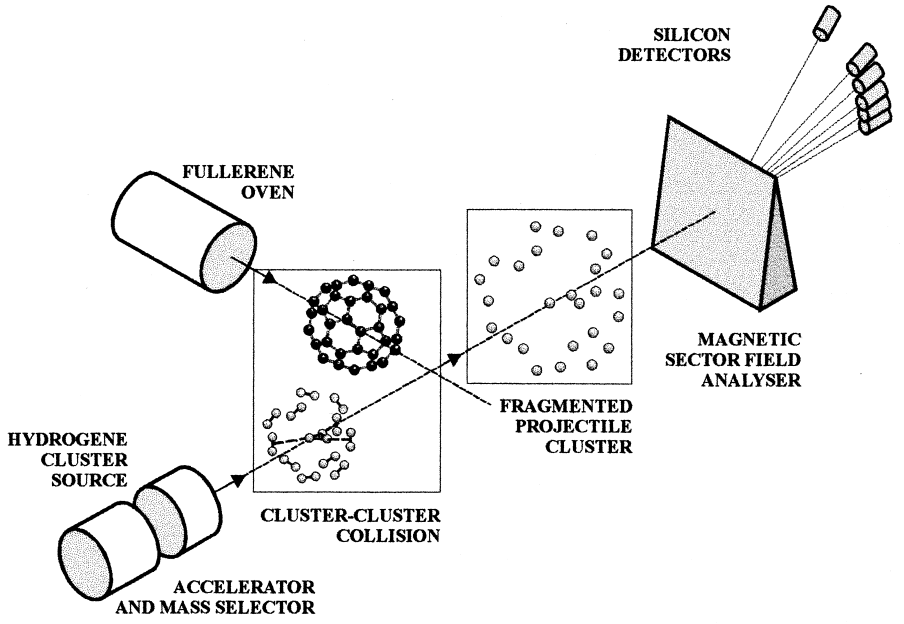

Fig. 1. Schematic view of the experimental setup. Mass selected hydrogen cluster ions of 60 keV/u energy are crossed perpendicularly by an effusive C_{60} beam in the collision region. Neutral and charged hydrogen fragments pass through a magnetic sector field analyzer one meter behind this collision region and are then detected in coincidence with a multidetector device consisting of a number of surface-barrier detectors located at different positions at the exit of the analyzer. For each fragmented cluster, the size and the number of the different fragments are recorded.

The fragmentation of H_{25}^+ with the helium target leads to a U-shaped fragment distribution [5]. This distribution is very different from the one obtained in low energy collision [8] where the yield of the fragment ions is observed to increase with the fragment size. Such behaviour observed here in the right part of the size distribution has usually been interpreted in the frame of the evaporative ensemble model. The main feature of the size distribution obtained in high energy cluster–atom collision is the prominent production of fragments of size that are intermediate ($3 \leq p \leq 13$) between the size of the evaporated dimers H_2 and the ones of the corresponding charged fragments.

In high energy cluster–cluster collision [9], fragmentation of H_{25}^+ clusters exhibits a monotonously decreasing distribution that is typical for the intermediate mass fragment (IMF) case known in nuclear physics. The increase at the higher p values present in the helium target case is not observed in collisions with C_{60}. This can be interpreted from the relative probability of the different energy depositions that can result from a collision. Indeed, on average, small charged fragments are due to violent collisions involving a large amount of energy transfer and large fragments are due to gentle types of interactions.

The presence of IMF in the size distributions could be interpreted by the occurrence of multifragmentation processes. Besides, in Fig. 2(b) the absolute cross section of fragment ions of size p (3 to $n - 2$, odd) resulting from the fragmentation of H_n^+ clusters ($n = 9, 13, 21, 25, 31$) colliding with helium at 60 keV/u are reported versus the normalized fragment size p/n. The discrepancy observed for $n = 9, 13$ is due to the choice of a scaling parameter that is not well suited when the value of the cluster size is small. The size distributions are found to be quite similar. In addition, specific features can be seen such as the fragment size 9, 19, etc. This can be related to the finite size effect such as geometrical shell effects in the structure of ionized hydrogen clusters.

Most importantly, as can be seen in a log–log plot

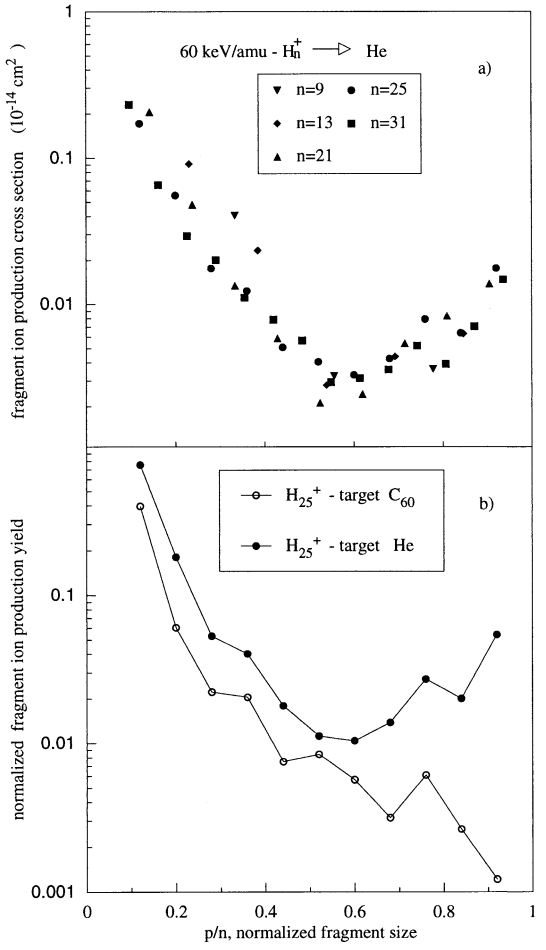

Fig. 2. Normalized cluster ion fragmentation distributions for hydrogen clusters. Upper part (a): Fragment ion cross section vs. normalized fragment size p/n for H_n^+ (n = 9, 13, 21, 25, 31) projectile ions interacting at 60 keV/u collision energy with a helium target. Lower part (b): Normalized fragment ion yield Y_p vs. normalized fragment size $p/25$ for H_{25}^+ projectile ions interacting at 1.5 MeV collision energy with a helium or C_{60} target, respectively.

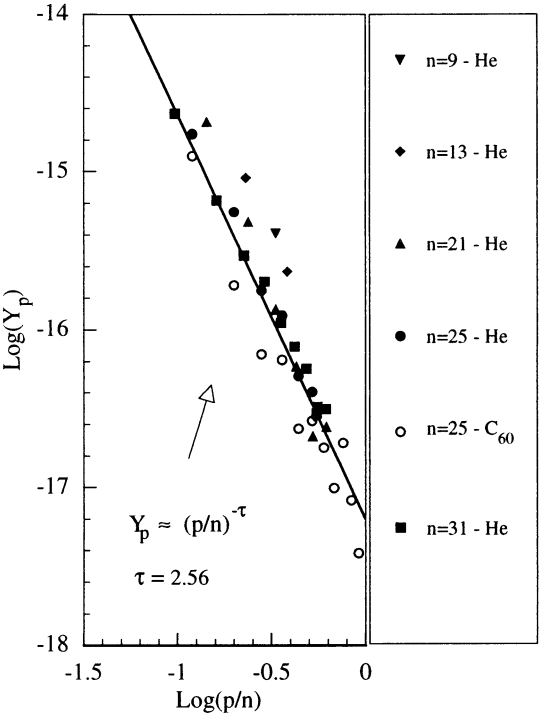

Fig. 3. Log–log plot of normalized fragment ion distributions for H_n^+ cluster ions interacting at 60 keV/u collision energy with a helium or C_{60} target.

of these data in Fig. 3, both the entire C_{60}–Y_p distribution and the left part of the He–Y_p ones ($p/n \leq 0.5$) follow a power law yielding a τ of 2.56 when fitting all the data (various sizes of clusters and various targets). Even more important, however, is that the present power law dependence is very similar to the IMF case in nuclear collision where the mass distribution follows a power law falloff with a τ value equal to 2.6 [10]. Moreover, there exists a strong similarity between the fragment size distribution and the predictions of certain models describing critical phenomena. The most famous is the Fisher droplet model [11] that allows one to calculate the droplet size distribution in a vapor. At the critical temperature the resulting distribution $f(p)$ in sizes p is proportional to $p^{-\tau}$ and the predicted exponent of 2.23 is close to the values observed for nuclear [10,12,13] and cluster fragmentations [14–16]. Although these observations have been taken as a strong hint for the occurrence of critical behaviour in a finite system reminiscent of a second order phase transition in an infinite system, it cannot be considered definitive proof.

4. Multi-ionisation, multifragmentation, and induced reaction in the cluster

In the velocity range studied here (1.55 times the Bohr velocity), electronic excitations up to ionisation

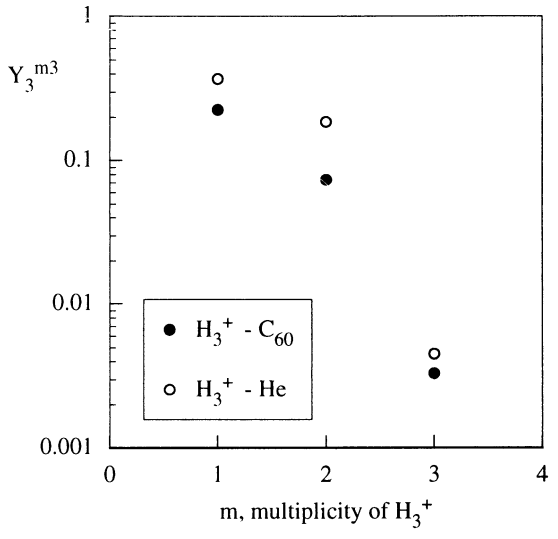

Fig. 4. Normalized H_3^+ fragment ion yield Y_3^{m3} vs. multiplicity m_3 of fragment ion production for H_{25}^+ projectile ions for a helium or C_{60} target.

of the incident cluster are involved in the collision. Moreover, the relative velocity of the projectile and the target atom is around or greater than the velocity of the electrons in the cluster. Then, the time for a typical collision with a target atom is short enough compared to the typical time of the motion of the protons in the cluster, so that during the collision the protons can be considered to be stationary in the projectile frame. Thus processes such as ionisation of the incident cluster followed by the fragmentation of the unstable multi-ionized cluster can be involved. As can be seen in Fig. 2 a prominent production of ionized fragments of intermediate sizes ($3 \leq p \leq 11$) are present in the size distributions. The first of these fragments is the protonated hydrogen H_3^+. Fig. 4 gives the normalized fragment ion yield Y_3^{m3} for the fragment ion H_3^+ for both target He and C_{60} where the multiplicity m_3 is the number of fragments H_3^+ produced per collision. Their relatively high value shows the importance of the ionization process. Y_3^{m3} is of the same order of magnitude for the two targets and both observed multiplicities reaching a value of three. Moreover, the fragmentation events with more than one H_3^+ demonstrated the multifragmentation process present in the data of the IMF size fragment ion distributions. This multiple production of H_3^+ has to be related to the high efficiency of the exothermic reaction $H_2^+ + H_2 \Rightarrow H_3^+ + H$. It has been studied at low energy [17] and the relative contribution of several competing channels are strongly dependent on the mass center collision energy and the initial vibrational states. It has been demonstrated that the production of H_3^+ predominates with an impact parameter smaller than 4 Å, the same order of magnitude than the close distance between the H_2 subunits in the cluster (few Å). Thus an important feature of these results is that high-energy cluster collision, cluster–cluster as well as cluster–atom collisions, can induce reaction in the cluster. There is recombination before fragmentation in the multi-ionized cluster and formation of H_3^+ ions that did not pre-exist in the incident cluster.

5. Large fluctuations inherent to phase transitions

Because percolation models have been used to simulate critical behaviour, they made their entrance into the description of multifragmentation. Besides the power law for the size distributions, percolation predicts certain properties associated with the various moment of the size fragment distributions. Bond percolation models have been used to describe nuclear fragmentation and to simulate critical behaviour predicting, besides the existence of a power law, additional properties of the fragment size distribution. These secondary characteristics (including Campi plots, multifactorial moment analysis, etc. [18–20]) are, however, only accessible via event by event data analysis as performed in the present experiment.

Thus, as an example following Campi [18] we plot and analyze the results H_{25}^+–C_{60} in the following way: in Fig. 5 (upper part) we plot the average size $P_{\max}$ of the largest fragment produced in a single event (normalized to the number of constituents, 25, in the primary hydrogen cluster ion projectile) versus the total number of fragments; this is called multiplicity m (normalized as done for $P_{\max}$ to the size of the system). In comparison we show the corresponding results obtained from a three-dimensional bond per-

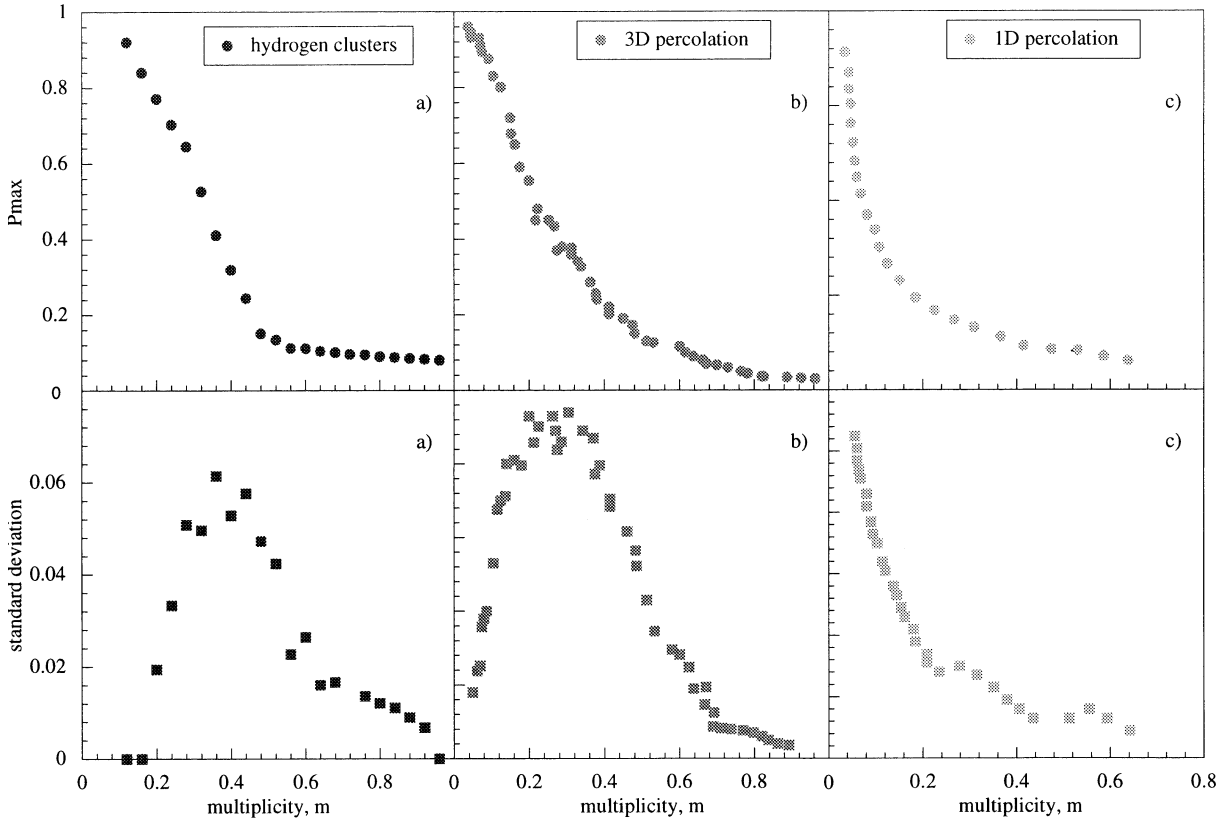

Fig. 5. Comparison of the fragmentation behaviour for three different systems: (a) hydrogen clusters, (b) three-dimensional (3D) bond percolation lattice, and (c) one-dimensional (1D) bond percolation lattice. In the cases of hydrogen clusters and three-dimensional bond percolation lattice, from the breakup in two fragments (low multiplicity) to the complete disintegration (high multiplicity), the fragmentation phenomenon exhibits a transition with an increase of the fluctuations. Upper part: Average size P_{max} of the largest fragment produced in a single event (normalized to the projectile size 25, to the number of sites 125 of the cubic lattice, or to the number of sites 125 of the linear lattice, respectively) vs. the normalized multiplicity m for the present experimental cluster fragmentation results, for the three-dimensional percolation model, and for the one-dimensional percolation model. Lower part: Normalized standard deviation (fluctuation) of P_{max} given in the upper part vs. m. The normalized standard deviation is defined as sqrt($\langle P_{max}$**2$\rangle - \langle P_{max}\rangle$**2).

colation model with 125 sites [18] [upper part of Fig. 5(b)] and a one-dimensional bond percolation model [upper part of Fig. 5(c)]. Because the fluctuations in fragment size distributions are largest near the critical point, it is interesting to also plot as a measure for these fluctuations the standard deviation of P_{max} versus the normalized multiplicity (lower part of Fig. 5). The following observations and points with respect to these results are noteworthy: (1) First of all there is a remarkable agreement in the overall shape of the functions obtained in the cluster–collision experiment on the one hand, and from the percolation model on the other hand. (2) The shift of the resonance-like peak in the standard deviation function is due to the size difference of the two systems.

We have to point out that for a one-dimensional percolation model [Fig. 5(c)] different results are obtained [18] with no resonance-like peak in the standard deviation function and therefore with no indication of a finite-size phase transition.

An experimental data set available for such an analysis of nuclear fragmentation, i.e. a nearly complete fragment charge analysis of 1 GeV/u Au ions bombarding an emulsion [21] of about 400 events [19], exhibits a similar behaviour [18] as the present cluster collision data and the three-dimensional per-

colation model. It should be mentioned, however, that according to DeAngelis et al. [19] this nuclear fragmentation data set is very likely biased towards low multiplicity events because the experimental setup records only those events in which all 79 charges are detected (see also another recent multifragmentation experiment with gold nuclei where the detector system permitted exclusive event reconstruction of nearly all charged reaction products [22]). In contrast, the present cluster collision experiment (with about 6000 events) includes all events and the comparison with the percolation model is unbiased from the detection probability.

The close resemblance between the results from percolation and the present cluster collision results constitutes a further step in ascertaining the occurrence of critical behaviour in these finite size collision systems: percolation is thought to provide a useful method to study phase transitions because of the similarities in the behaviour with systems exhibiting second order phase transitions, such as liquid–vapor systems at the critical temperature [23]. A particular advantage of this comparison is the fact that according to Campi [24] it is possible to compare in this way nuclear collision (and also cluster collision) data with results of percolation on finite size lattices of a similar size and thus avoid the problem of the finite size of these systems.

6. Conclusion

This experimental study of cluster fragmentation is novel because of the possibility of observing the fragmentation phenomenon in the same conditions for a large range of energy deposited. From a small amount of energy transfer in the "gentle collisions" inducing the loss of one cluster component up to a large amount of energy transfer in the "violent collisions" inducing complete cluster disintegration, we observe a transition with an increase of the fluctuations. The critical region corresponding to an increase of the fluctuations is connected to the observation of a recombination in the cluster after multi-ionization. Indeed, there is an excitation range for which there is a kind of "chemical reaction" and formation of fragments which did not pre-exist in the structure components of the cluster before the collisional interaction.

From a general point of view, quite different objects such as nuclei and molecular clusters show similar fragmentation behaviour not only in the inclusive fragment size distribution but also in the event by event type analysis. This is in accordance with a recent scaling prediction concerning large fluctuations in finite systems [20,25]. The application of the predicted characterizations of fragment size distributions [26] is demonstrated here for cluster fragmentation data (see also a theoretical study by Lutz and co-workers [27]). However, besides the usefulness of this approach for microscopic systems like nuclei (fermi scale) or clusters (nanometer scale) it might also be applicable on a more universal scale including macroscopic phenomena.

Acknowledgements

Most of the results that have been reported were obtained in collaboration with other groups and visitors. We would like to sincerely thank P. Scheier, G. Senn, T. D. Märk, J.P. Buchet, M. Carré, G. Jalbert, N.V. de Castro Faria, and F. Gobet.

References

[1] D. Beyson, X. Campi, E. Pefferkorn (Eds.), Fragmentation Phenomena, World Scientific, Singapore, 1995.
[2] I. Stich, D. Marx, M. Parrinello, K. Terakura, J. Chem. Phys. 107 (1997) 9482.
[3] I. Stich, D. Marx, M. Parrinello, K. Terakura, Phys. Rev. Lett. 78 (1997) 3669.
[4] M. Farizon, H. Chermette, B. Farizon-Mazuy, J. Chem. Phys. 96 (1992) 1325.
[5] B. Farizon, M. Farizon, M.J. Gaillard, E. Gerlic, S. Ouaskit, Nucl. Instrum. Methods Phys. Res. B 88 (1994) 86.
[6] B. Farizon, M. Farizon, M.J. Gaillard, E. Gerlic, R. Genre, S. Louc, N.V. de Castro Faria, G. Jalbert, Chem. Phys. Lett. 252 (1996) 147.
[7] B. Farizon, M. Farizon, M.J. Gaillard, E. Gerlic, S. Ouaskit, Nucl. Instrum. Methods. Phys. Res. B 101 (1995) 287.
[8] A. Van Lumig, J. Reuss, Int. J. Mass Spectrom. Ion Phys. 27 (1978) 197.
[9] B. Farizon, M. Farizon, M.J. Gaillard, Int. J. Mass Spectrom. Ion Processes 164 (1997) 225.

[10] A.S. Hirsch, A. Bujak, J.E. Finn, L.J. Gutay, R.W. Minich, N.T. Porile, R.P. Scharenberg, B.C. Stringfellow, Phys. Rev. C 29 (1984) 508.
[11] M.E. Fisher, Rep. Prog. Phys. 30 (1967) 615.
[12] X. Campi, Nucl. Phys. A 495 (1989) 259c.
[13] V. Latora, M. Belkacem, A. Bonasera, Phys. Rev. Lett. 73 (1994) 1765.
[14] T. LeBrun, H.G. Berry, S. Cheng, R.W. Dunford, H. Esbensen, D.S. Gemmell, E.P. Kanter, W. Bauer, Phys. Rev. Lett. 72 (1994) 3965.
[15] J. Schulte, Phys. Rev. B 51 (1995) 3331.
[16] P. Scheier, B. Dünser, R. Wörgötter, S. Matt, D. Muigg, G. Senn, T.D. Märk, Int. Rev. Phys. Chem. 15 (1996) 93.
[17] J.E. Pollard, L.K. Johnson, P.A. Lichtin, R.B. Cohen, J. Chem. Phys. 95 (1991) 4877.
[18] X. Campi, Phys. Lett. B 208 (1988) 351.
[19] A.R. DeAngelis, D.H.E. Gross, R. Heck, Nucl. Phys. A 537 (1992) 606 and references therein.
[20] M. Belkacem, V. Latora, A. Bonasera, Phys. Rev. C 52 (1995) 271.
[21] C.J. Waddington, P.S. Freier, Phys. Rev. C 31 (1985) 888.
[22] M.L. Gilkes et al., Phys. Rev. Lett. 73 (1994) 1590.
[23] L.G. Moretto, G.J. Wozniak, Annu. Rev. Nucl. Sci. 43 (1993) 379.
[24] X. Campi, J. Phys. A 19 (1986) L917.
[25] A. Bonasera, J. Schulte, Report MSUCL, 966, Michigan State University, 1995.
[26] X. Campi, H. Krivine, Observables in Fragmentation, in [1].
[27] V.N. Kondratyev, H.O. Lutz, Z. Phys. D 40 (1997) 210.